

Author [Krupanidhi, S. B.](#); [Hudait, M. K.](#)

Author Affiliation Mater. Res. Centre, Indian Inst. of Sci., Bangalore, India

Title Interface characterization of GaAs/Ge heterostructure grown by metalorganic vapor phase epitaxy

Appears In [Proceedings of the SPIE - The International Society for Optical Engineering](#). vol.3975, pt.1-2 2000. p. 171-8.

Journal Abbr. Proc. SPIE - Int. Soc. Opt. Eng. (USA)

Conference Tenth International Workshop on the Physics of Semiconductor Devices. New Delhi, India. 14-18 Dec. 1999.

Publisher SPIE-Int. Soc. Opt. Eng , 2000.

Abstract GaAs/Ge heterostructures having abrupt interfaces were grown under different growth conditions and investigated by atomic force microscopy (AFM), cross sectional high resolution transmission electron microscopy (HRTEM), low temperature photoluminescence (LTPL) spectroscopy, electrochemical capacitance voltage (ECV) profiling and current/voltage (I/V) characteristics. Our results indicate that a 6 degrees off cut Ge substrate coupled with a growth temperature of ~675 degrees C, growth rate of ~3 $\mu\text{m/hr}$ and a V/III ratio of ~88 is an optimum growth condition for the buffer layer growth of GaAs/Ge heterostructure solar cells. The surface morphology was found to be very good on 6 degrees off oriented Ge substrate and rms roughness was ~30.8 nm over $10 * 10 \mu\text{m}^2$ area scan over 2 degrees and 9 degrees off oriented Ge substrates. The lattice indexing of HRTEM exhibited an excellent lattice line matching between GaAs and Ge substrates. The ECV profiler shows an excellent abruptness between the film/substrate interface of GaAs/Ge and also between various layers of the complete solar cell structures. Finally, the I/V characteristics of GaAs/Ge solar cells were analysed under AM0 condition. Abstract no. A2001-10-6848-002B2001-05-2530B-017.

Identifiers heterostructure solar cells. metalorganic vapor phase epitaxy. MOVPE. interface characterization. atomic force microscopy. AFM. high resolution transmission electron microscopy. HRTEM. low temperature photoluminescence. LTPL spectroscopy. electrochemical capacitance voltage profiler. ECV. current/voltage characteristics. optimum growth condition. buffer layer growth. surface morphology. lattice indexing. lattice line matching. AM0 condition. 67 degC. GaAs-Ge. Ge

Subjects [atomic force microscopy](#)
[capacitance](#)
[gallium arsenide](#)

[germanium](#)
[III-V semiconductors](#)
[interface roughness](#)
[MOCVD](#)
[photoluminescence](#)
[semiconductor heterojunctions](#)
[solar cells](#)
[transmission electron microscopy](#)

Classification [A6848](#) ; [A7340L](#) ; [A6855](#) ; [A8115H](#) ; [A8630J](#) ; [A7855E](#) ; [B2530B](#) ;
Codes [B2520D](#) ; [B8420](#) ; [B0520F](#)

Chemical GaAs-Ge/int GaAs/int As/int Ga/int Ge/int GaAs/bin As/bin Ga/bin
Indexing Ge/el. Ge/sur Ge/el

Numerical temperature 3.40E+02 K
Indexing

Material C574-2000-225
Identity No.

Record Type Conference Paper

Number of 29
References

ISSN 0277-786X

CODEN PSISDG

SICI 0277-786X(2000)3975:1/2L.171:ICGH;1-I

Treatment Experimental

Language English

Country of USA
Publication

INSPEC 6888428
Accession
Number

Interface Characterization of GaAs/Ge Heterostructure Grown by Metal-Organic Vapor-Phase Epitaxy

S. B. Krupanidhi¹ and M. K. Hudait,^{1,2}

¹ *Materials Research Centre, Indian Institute of Science, Bangalore 560 012, INDIA*

² *Central Research Laboratory, Bharat Electronics, Bangalore 560 013, INDIA*

ABSTRACT

GaAs/Ge heterostructures having abrupt interfaces were grown under different growth conditions and investigated by atomic force microscopy (AFM), cross-sectional high resolution transmission electron microscopy (HRTEM), low-temperature photoluminescence (LTPL) spectroscopy, electrochemical capacitance voltage (ECV) profiler and current-voltage (I-V) characteristics. Our results indicate that 6° off-cut Ge substrate coupled with growth temperature of ~ 675°C, growth rate of ~ 3 μm/hr and a V/III ratio of ~ 88 is an optimum growth condition for the buffer layer growth of GaAs/Ge heterostructure solar cells. The surface morphology was found to be very good on 6° off-oriented Ge substrate and rms roughness was ~ 30.8 nm over 10 × 10 μm² area scan over 2° and 9° off-oriented Ge substrates. The lattice indexing of HRTEM exhibited an excellent lattice line matching between GaAs and Ge substrates. The ECV profiler shows an excellent abruptness between the film/substrate interface of GaAs/Ge and also between various layers of the complete solar cell structures. Finally, the I-V characteristics of GaAs/Ge solar cells were analysed under AM0 condition.

1. INTRODUCTION

GaAs/Ge heterostructures (HSs) have received a great attention as starting materials for the fabrication of space quality solar cells [1-5]. Due to its high mechanical strength, Ge is an optimized substrate material for high efficiency solar cells [6, 7]. Although the low lattice mismatch (0.07%) of the GaAs/Ge system suggests it should be nearly dislocation free, polar-on-nonpolar heteroepitaxy poses several unique problems, like misfit dislocations at the interface, APDs in the polar materials, and the cross diffusion of Ga, As and Ge at the GaAs/Ge heterointerface. The APDs separated by APBs in the III-V compound semiconductors are harmful for devices, which are based on the heterointerface properties, since the APBs act as nonradiative recombination centers [8, 9]. To avoid the formation of APDs, harmful to GaAs/Ge solar cell performance as they reduce short-circuit current, misoriented substrates were used by several authors. Another problem is the Ga diffusion into the Ge substrate, which results in unwanted p-n junction at the GaAs/Ge heterointerface or inside the Ge substrate that could affect the performance of the GaAs/Ge solar cell [3]. Therefore, the careful control of the substrate surface structure and the initial growth conditions, like the initial growth temperature, growth rate and the V/III ratio [10-13] are essential to grow device quality single-domain GaAs/Ge heterostructures.

In the present work, we have investigated the effect of off-orientation, growth temperature, V/III ratio and growth rate on metal-organic vapor-phase epitaxy (MOVPE) grown Si-doped n-type GaAs on Ge substrates for solar cell application. The study leads to establishment of optimum growth conditions,

which reproducibly generate APD-free n-type GaAs films on Ge and limit outdiffused Ge concentration at the GaAs/Ge heterointerface. The efforts dedicated to find out the proper growth conditions have allowed us to obtain higher conversion efficiency under AMO condition on large area GaAs/Ge solar cells by low-pressure metal-organic vapor phase epitaxy (LP-MOVPE). Atomic force microscopy (AFM) and low temperature photoluminescence (LTPL) spectroscopy were used for characterizing the n-GaAs epilayers. The GaAs/Ge interface was characterized using high-resolution transmission electron microscopy (HRTEM) and electrochemical capacitance-voltage (ECV) profiling. After optimizing the growth conditions for the buffer layer growth of Si-doped GaAs on Ge substrate, GaAs/Ge solar cells were grown and characterized using LTPL, ECV profiler and current-voltage (I-V) measurements.

2. Experimental

The Si-doped n-type GaAs films were grown in a low-pressure horizontal MOVPE reactor on Si-doped n⁺-Ge (100) 2°, 6° and 9° off-oriented towards [110] direction. The source materials were trimethylgallium (TMGa), 100% arsine (AsH₃), trimethylaluminum (TMAI), dimethylzinc (DMZn) as a p-type dopant, 104 ppm silane (SiH₄) as an n-type dopant and palladium purified H₂ as a carrier gas. The details of the growth procedure can be found elsewhere [13-16].

The thickness of the epitaxial layers investigated ranged from about 1.5 μm to 6.5 μm. The epitaxial films were investigated using AFM to reveal the surface roughening and other defects, probably APDs, in a constant-force mode. The epitaxial GaAs/Ge heterointerfaces were prepared by Ar⁺ ion thinning for cross-sectional observations. The HRTEM investigations were performed using a Hitachi H-9000 UHR ultra-high resolution electron microscope operated at 300 kV. PL measurements were carried out using a MIDAC Fourier Transform PL (FTPL) system at a temperature of 4.2 K and 100 mW laser power. Argon ion laser operating at a wavelength of 5145 Å was used as a source of excitation. The exposed area was about 3 mm². PL signal was detected by a LN₂ cooled Ge-Photodetector whose operating range is about 0.75-1.9 eV. The doping concentrations were determined using Bio-Rad ECV polaron profiler.

The metal front contact on GaAs/Ge solar cell structure was made using Au:Zn and an overlayer of Au using a physical mask on the GaAs epilayer and annealed at 450°C for about 2 min in ultra high pure (UHP) N₂ ambient. The thickness of the front metal contact was about 0.35 μm. The cap layer was etched using H₃PO₄:H₂O₂:H₂O (10:10:394) for about 7-8 min depending on the thickness of the metal grid to reduce the series resistance effect on the solar cell efficiency. Once the cap layer was etched, an AR coating consisting of TiO₂ and Al₂O₃ double layer, having thickness of about 370 Å and 500 Å, respectively, was deposited on top of the window layer. The current-voltage (I-V) measurement were carried out using Oriol Solar Simulator and an automated setup consisting of Keithley 2400 source measure unit, probe station and an IBM 486 PC.

3. RESULTS AND DISCUSSION

3.1 Surface characterization by AFM Studies

The careful control of substrate surface structure is essential to realize the APD-free GaAs on different off-oriented Ge substrates by MOVPE technique. In general, the surface roughening in GaAs films on Ge substrates by MOVPE growth process is mainly due to APDs [17, 18]. AFM images on different length scales have been taken to see the top surface morphology of the epitaxial Si-doped GaAs films on off-oriented Ge substrates as a function of growth temperature (600 °C – 700 °C) and the effect of off-orientation (2°, 6° and 9°). However, we are reporting here the surface morphology only on the 6° off-oriented Ge substrates. One of the AFM images of a small area scan is shown in Fig. 1 with a growth temperature of 675°C, V/III ratio of 88.20 and a growth rate of 3 μm/hr. The film grown at 675°C shows reasonably low average and rms roughness value and has better surface morphology compared with the films grown at other temperature [19]. The average roughness was determined from the scan over the top

of the films of different area scan. The surface morphology was found to be very good on 6° off-oriented Ge substrate and the rms roughness was ~ 30.82 nm over $10 \times 10 \mu\text{m}^2$ area scan compared to 2° and 9° off-oriented Ge substrates.

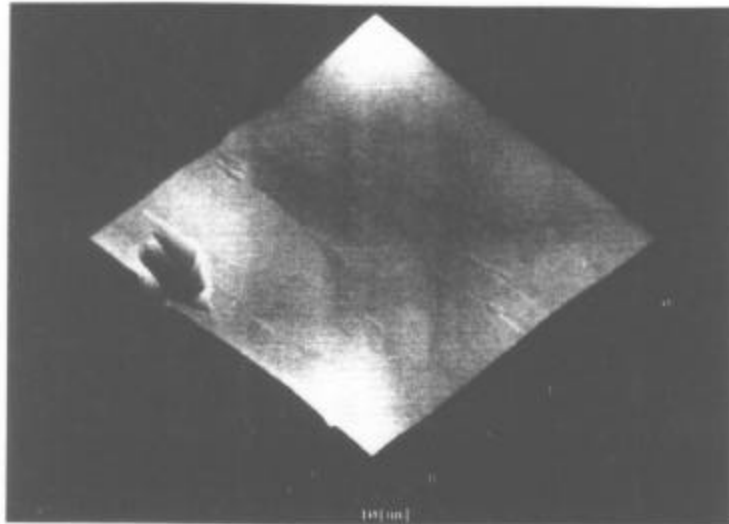


Fig. 1 Topographical image of the $1.5 \mu\text{m}$ thick Si-doped GaAs epilayer grown on 6° off-oriented Ge substrate with a growth rate of $3 \mu\text{m/hr}$, V/III ratio of 88.20 and a growth temperature of 675°C

Growth at too low temperature results in excess As point defects, which nucleate dislocation loops. These loops expand during the subsequent high temperature GaAs growth to generate high threading dislocation densities in the thick GaAs film [20]. On the other hand, the growth at higher temperature and lower growth rate may result in the formation of unwanted p-n junction due to simultaneous indiffusion of Ga and As inside the Ge substrate, which in turn reduces the solar cell efficiency [3]. Based on this study we can conclude that 6° off-oriented Ge substrate coupled with a V/III ratio of $\sim 88:1$ and a growth rate of $\sim 3 \mu\text{m/hr}$ is the optimum growth condition for the buffer layer growth of Si-doped GaAs on Ge substrate.

3.2 Interface Characterization

3.2.1 Cross-sectional High resolution Transmission Electron Microscopy Studies on GaAs/Ge Heterointerfaces

The epitaxial films were investigated by TEM to reveal the characteristics of MDs and other crystalline defect [21]. In general, the dominant crystalline defects observed in the GaAs epi-film grown on Ge are APDs and dislocations. Fig. 2 shows the cross-sectional high-resolution TEM image of GaAs on Ge substrates in an atomic scale, using an As prelayer, growth temperature of 675°C , V/III ratio of 88.20 and a growth rate of $3 \mu\text{m/hr}$. It can be seen that for the layer grown under these growth conditions, the interface between the GaAs epilayer and the Ge substrate is sharp and no APDs were observed at the heterointerface. The epitaxial growth of GaAs and Ge substrate is clearly visible in this high-resolution image with the well-resolved GaAs lattice lines extending all the way down to the Ge surface closely matching with the Ge lattice. From our cross-sectional HRTEM observation on the GaAs/Ge heterointerface, we can conclude that the growth temperature of 675°C and growth rate of $3 \mu\text{m/hr}$ in the LP-MOVPE process is the main growth condition for APD-free GaAs on 6° offcut Ge substrate, which is in agreement with the AFM study.

3.2.2 Electrochemical Capacitance-Voltage Profile

The Bio-Rad ECV profiler was used to determine the concentration along depth in the Si-doped GaAs on different off-oriented Ge substrates. Fig. 3 shows one of the ECV carrier concentration profiles of Si-doped GaAs on Ge substrates of 2°, 6° and 9° off-orientation. The GaAs/Ge heterointerface for 6° off-orientation is found to be extremely abrupt as compared to other off-orientations in the same growth conditions. It can be also noticed that there is no p-n junction formation due to simultaneous indiffusion of Ga and As into Ge in all the off-orientations during the MOVPE growth process. The carrier concentration is uniform along the depth in 6° and a clear GaAs/Ge interface was observed in all the present investigated films. From this figure, we can infer that the 6° off-oriented Ge substrate is a proper choice for the GaAs/Ge heterojunction solar cells application under our present growth conditions.

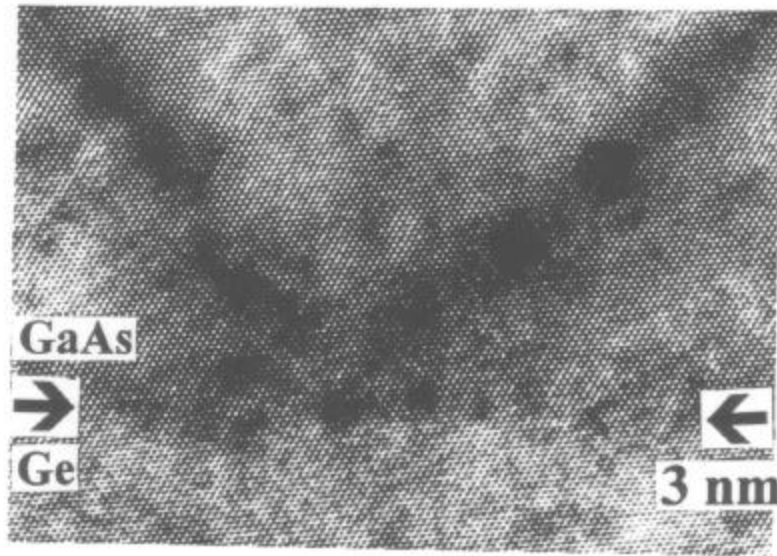


Fig.2 [110] cross-sectional high-resolution TEM image of heterointerface of GaAs/(100) Ge heterostructure.

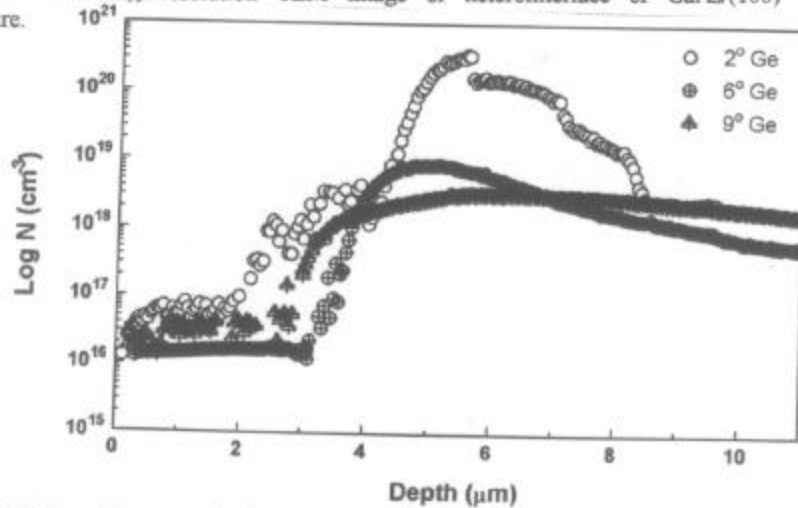


Fig.3 ECV profile of Si-doped GaAs on 2°, 6° and 9° off-oriented Ge substrates.

3.2.3 Effect of Variation of Growth Temperature on Carrier Concentration

The electron concentration is observed to increase as the growth temperature increases, as shown in Fig. 4 for a fixed SiH_4 mole fraction. The activation energy for doping (E_a) can be determined from Fig. 4. The activation energy of Si in GaAs ranges from 3.5 eV to 4.13 eV on the different off-oriented Ge substrates. This value is significantly higher (about a factor of 3) than Si-doped GaAs on GaAs substrates reported in literature [22-24] using SiH_4 as an n-type dopant. The strong temperature dependence of Si incorporation is believed to be a result of increasing decomposition rate of SiH_4 with increasing temperature. From this figure one can observe that at any given temperature, the change in carrier concentration with off-oriented Ge substrates is significantly small.

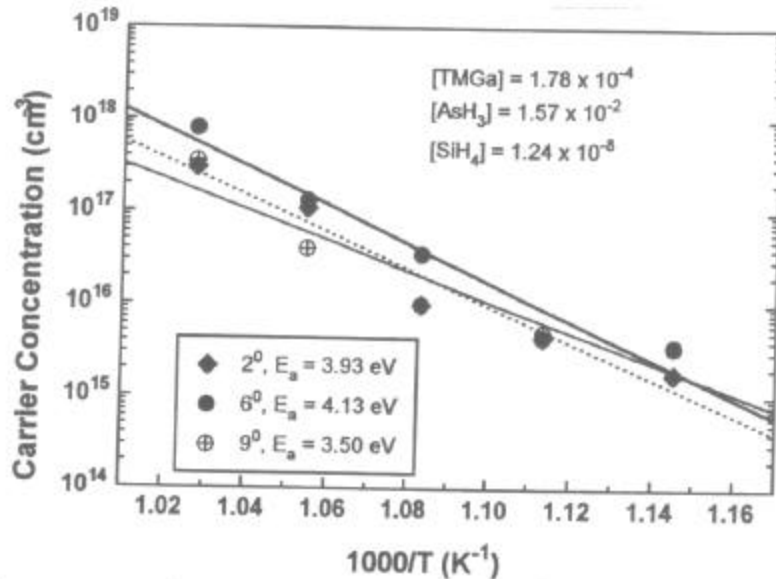


Fig.4 Electron concentration vs growth temperatures on 2°, 6° and 9° off-oriented Ge substrates.

3.2.4 Optical Properties on Different Off-oriented Ge Substrates

Fig. 5 shows the PL spectra obtained from the Si-doped GaAs epilayers on 2°, 6° and 9° off-oriented Ge substrates grown at a substrate temperature of 675 °C. When the electron concentration is relatively low, the PL spectrum is symmetric while higher concentration leads to asymmetric spectrum. The Si doping broadens the excitonic emission until it becomes a wide band-to-band (B-B) luminescence. The peak at around 1.49 eV has been attributed to band-to-acceptor (B-A) transitions involving residual carbon (C) impurities present in MOVPE GaAs [25]. The energy separation between the B-A peak and the B-B peak (band gap of GaAs at 4.2 K is 1.5194 eV) is consistent with typical acceptor ionization energies such as that of C ($E_a \sim 26.4$ meV) [26], which is a p-type dopant in MOVPE. The B-A transitions were observed from all the off-oriented Ge substrates and the peak intensity due to C decreases with the growth temperatures compared with the excitonic peak intensity for all the off-oriented Ge substrates. The peak intensity due to excitonic transitions are higher than C-related transitions on 6° and 9° off-oriented Ge substrates, whereas on 2° off-oriented Ge substrate, the intensity of the two peaks are almost same. Therefore, the 6° or 9° Ge substrate would be the proper choice for growth of Si-doped GaAs by LP-MOVPE process. At 675°C, the excitonic peak intensity is higher than the peak intensity due to carbon in all the three orientations. The doping profile of Si-doped GaAs on 2°, 6° and 9° off-oriented

Ge substrates were shown in Fig. 3. Therefore, in our present growth conditions an optimum off-orientation of Ge substrate for the space quality solar cells is 6° .

3.3 GaAs/Ge Solar Cell Characterization

3.3.1 Optical Characteristics of Solar Cells

Optical characterization of the complete solar cell was carried out using LTPL spectroscopy at 4.2 K measurement temperature. Fig. 6 shows the experimental PL spectra of GaAs/Ge 6° and GaAs/Ge 9° structures measured at 4.2 K. The interference effects from different layers are not observed in this PL spectrum. If it is present then there should be the secondary peak (s) along with the main emission peak [27, 28]. Since there are no secondary peaks present in the PL spectrum, we can consider that the main emission comes from the top of the film or from the cap and emitter layers. The luminescence efficiency from GaAs/Ge solar cell grown on 9° off-oriented Ge substrate is very low as compared to the luminescence efficiency from GaAs/Ge solar cell grown on 6° off-oriented Ge substrates. From this observation one can rule out the possibility of growing solar cells on 9° off-oriented Ge substrates. Therefore, the selection of the 6° off-oriented Ge substrate for the GaAs/Ge heterostructure solar cells is justified not only from the PL study of the complete solar cell structure but also from AFM and HRTEM studies.

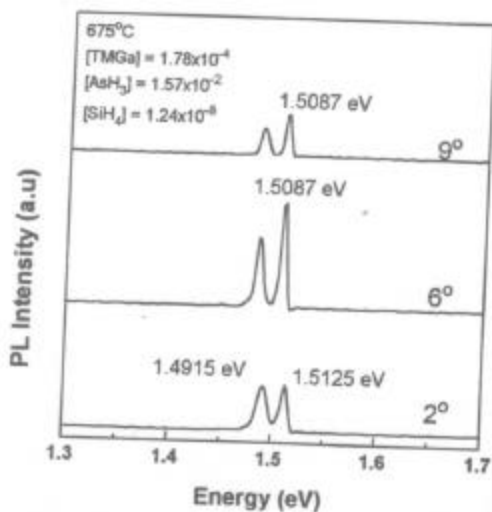


Fig.5 PL spectra of Si-doped GaAs epilayers grown on 2° , 6° and 9° off-oriented Ge substrates.

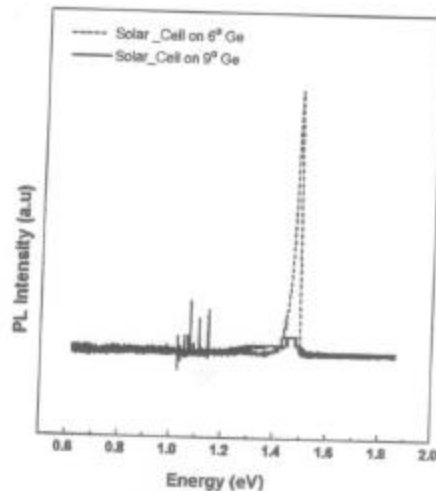


Fig.6 4.2 K PL spectra of GaAs solar cell grown on 6° and 9° off-oriented Ge substrates.

3.3.2 Electrochemical Capacitance-Voltage Profiles of GaAs/Ge Solar Cell Structure

To gain a fundamental understanding of the performance of multi-layered GaAs/Ge solar cell, ECV profiling was used to examine the depth profile of the carrier concentration in each layer, thickness of each layer and the abruptness between the two layers. Figure 7 shows one of the ECV profiles of GaAs/Ge heterostructure solar cell with controlled interfaces between the two adjacent layers. One can carefully control the MOVPE growth parameters for obtaining a highly abrupt interface between the emitter and base layer of the GaAs/Ge solar cell. The GaAs and AlGaAs interface is very abrupt. During

the growth of complete solar cell structure, we had increased or decreased the n-type and p-type dopants input mole fractions depending on the carrier concentration requirement in each layer. Also, the duration of each layer was adjusted prior to the growth rate knowledge of each dopant. We did not observe any p-n junction formation inside the Ge substrate during the growth of complete solar cell structure.

3.3.3 Current-Voltage Characteristics of Solar Cells

Figure 8 shows the I-V characteristics of one of the 1 cm x 1 cm solar cell on the GaAs/Ge 6° substrate under AM0 condition. The efficiency of the solar cell is 12.42 % with a V_{oc} of 0.955 V, J_{sc} of 27.43 mAcm⁻² and FF of 0.64 (with a front metal contact of 0.35 μm). Based on our experimental investigations, the FF should improve to above 0.8, when the front contact layer thickness is made 5 μm [29]. If we consider that the FF is 0.75, the solar cell efficiency is 14.55 % and for FF of 0.8 the efficiency is 15.52 %. In our case, the metal coverage area was 30 %, since the cell was made using physical mask during thermal evaporation, as the devices are meant for a nominal characterization. Generally the metal coverage area is 5 to 10 %. After considering the extra effect of metal grid contact (extra 20 %) the efficiency will improve to 18.2 % (FF = 0.75) and 19.4 % (FF = 0.8).

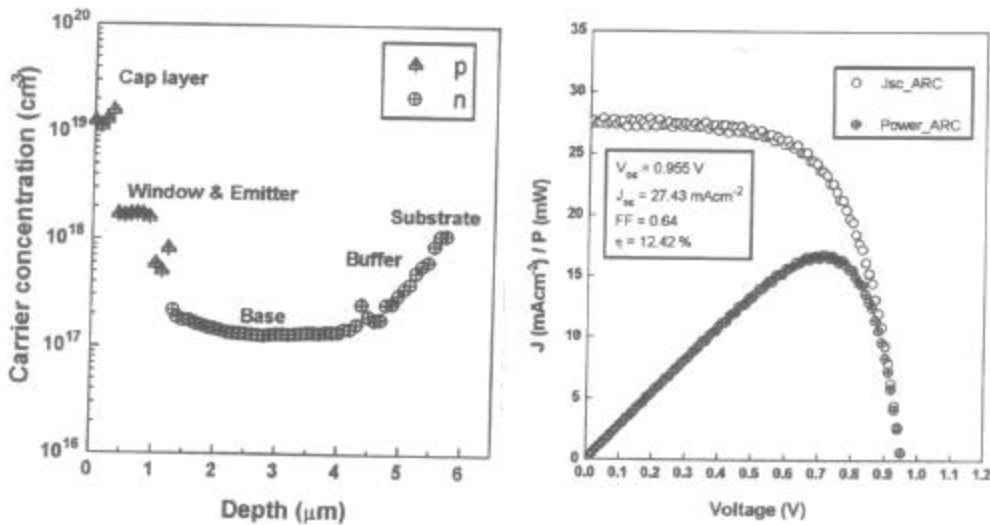


Fig.7 ECV profile of GaAs/Ge6° heterostructure solar cell.

Fig.8 Current density and power vs voltage characteristics of GaAs/Ge6° heterostructure solar cell. The open circuit voltage (V_{oc}), short current density (J_{sc}), Fill Factor (FF) and efficiency (η) are given.

4. CONCLUSIONS

The Si-doped GaAs epitaxial layers on different off-oriented Ge substrates were grown by LP-MOVPE growth technique and characterized by several characterization techniques. AFM studies show that the film grown at 675°C and 3 μm/hr growth rate has better surface morphology on 6° compared with 2° and 9° off-oriented Ge substrates. Using HRTEM, we have identified the optimum growth parameters, which can reproducibly generate APD-free GaAs on Ge by MOVPE growth process. The ECV profile of Si-doped GaAs on 6° off-oriented Ge substrate shows abrupt GaAs/Ge heterointerface. The excitonic

luminescence efficiency from the Si-doped GaAs epitaxial film on 6° and 9° off-oriented Ge substrates is greater than that from 2° off-oriented Ge substrate. The LTPL spectra on the GaAs solar cell structure show very less luminescence intensity on 9° off-oriented Ge substrate and it is not suitable for the space quality solar cell applications. The ECV profile of GaAs/Ge 6° heterostructure shows excellent abruptness between each layer. The GaAs/Ge 6° heterostructure solar cells shows the efficiency greater than 18 % after considering the effects of thick metal layer and the low grid coverage ratio. This clearly establishes the device quality of GaAs layers with different dopants, doping concentrations and abrupt interfaces between each layer, which can reproducibly allow us to obtain efficiency greater than 18 %.

REFERENCES

- [1] R. A. Metzger, *Compound Semicond.*, **2**, 25 (1996).
- [2] K.I. Chang, Y. C. M. Yeh, P. A. Iles, J. M. Tracy, R. K. Morris, *Proc. 19 th IEEE Photovolt. Spec. Conf.* (1987) p. 273.
- [3] P. A. Iles, Y. C. M. Yeh, F. H. Ho, C. L. Chu, and C. Cheng, *IEEE Electron Device Lett. EDL-11*, 140 (1990).
- [4] T. Whitaker, *Compound Semicond.*, **4**, 32 (1998).
- [5] J. C. Chen, M. L. Ristow, J. I. Cabbage, and J. G. Werthen, *J. Electron. Mater.* **21**, 347 (1992).
- [6] C. Flores, B. Bollani, R. Campensato, D. Passoni, and G. L. Timo, *Microelectron. Eng.* **18**, 175 (1992).
- [7] S. J. Wojtczuk, S. P. Tobin, C. J. Keavney, C. Bajgar, M. M. Sanfacon, L. M. Geoffroy, T. M. Dixon, S. M. Vernon, J. D. Scofield, and D. S. Ruby, *IEEE Trans. Electron Device ED-37*, 455 (1990).
- [8] H. Kroemer, *J. Crystal Growth* **81**, 193 (1987).
- [9] P. M. Petroff, *J. Vac. Sci. Technol. B* **4**, 874 (1986).
- [10] Y. Li, L. Lazzarini, L.J. Giling, and G. Salviati, *J. Appl. Phys.* **76**, 5748 (1994).
- [11] Y. Li, G. Salviati, M. M. G. Bongers, L. Lazzarini, L. Nasi, and L.J. Giling, *J. Crystal Growth* **163**, 195 (1996).
- [12] Y. Li and L. J. Giling, *J. Crystal Growth* **163**, 203 (1996).
- [13] M. K. Hudait and S. B. Krupanidhi, *J. Appl. Phys.* (submitted) 1999.
- [14] M. K. Hudait, P. Modak, S. Hardikar, and S. B. Krupanidhi, *J. Appl. Phys.* **83**, 4454 (1998).
- [15] M. K. Hudait, P. Modak, S. Hardikar, K. S. R. K. Rao, and S. B. Krupanidhi, *Mat. Sci. Eng. B* **55**, 53 (1998).
- [16] P. Modak, M. K. Hudait, S. Hardikar, and S. B. Krupanidhi, *J. Crystal Growth* **193**, 501 (1998).
- [17] Q. Xu, J. W. P. Hsu, S. M. Ting, E. A. Fitzgerald, R. M. Seig, and S. A. Ringel, *J. Electron. Mater.* **27**, 1010 (1998).
- [18] Q. Xu and J. W. P. Hsu, *J. Appl. Phys.* **85**, 2465 (1999).
- [19] M. K. Hudait and S. B. Krupanidhi, *Mat. Res. Bulletin* (in press, 1999).
- [20] S. M. Ting, E. A. Fitzgerald, R. M. Sieg, and S. A. Ringel, *J. Electron. Mater.* **27**, 451 (1998).
- [21] M. K. Hudait and S. B. Krupanidhi, *Mat. Res. Bulletin*, (in press, 1999).
- [22] T. F. Kuech, E. Veuhoff, and B. S. Meyerson, *J. Crystal Growth* **68**, 48 (1984).
- [23] S. J. Bass, *J. Crystal Growth* **47**, 613 (1979).
- [24] J. P. Duchemin, M. Bonnet, F. Koelsch, and D. Huyghe, *J. Electrochem. Soc.* **126**, 1134 (1979).
- [25] V. Swaminathan, D. L. Van Haren, J. L. Zilko, P. Y. Lu, and N. E. Schumaker, *J. Appl. Phys.* **57**, 5349 (1985).
- [26] D. J. Ashen, P. J. Dean, D. T. J. Hurle, J. B. Mullin, and A. M. White, *J. Phys. Chem. Solids* **36**, 1041 (1975).
- [27] G. L. Timo and C. Flores, *1 st World Conf. Photovolt. Energy Conver., Hawaii*, (1994) p. 2200.
- [28] M. Yang, M. Yamaguchi, T. Takamoto, E. Ikeda, H. Kurita, M. Ohmori, *Solar Cells Materials and Solar Cells* **45**, 331 (1997).
- [29] M. A. Green, *Solar Cells, Operating Principles, Technology, and System Applications*, (Prentice-Hall, NJ, 1982).